A95- 36589 AIAA-95-1738-CP

Flux Limited Dissipation Schemes for High Speed Unsteady Flows

*Chong Am Kim** *and Antony Jameson*†
Department of Mechanical and Aerospace Engineering
Princeton University
Princeton, New Jersey 08544 U.S.A.

Abstract

Within the framework of the Local Extremum Diminishing (LED) or Essentially Local Extremum Diminishing (ELED) principle, efficient approaches to obtain a class of non-oscillatory high resolution schemes are presented. The LED principle requires that local maxima should not increase and local minima should not decrease to produce a monotonicity preserving scheme for scalar hyperbolic conservation laws. The LED constraint can be judiciously relaxed by the ELED approach to achieve high accuracy at smooth extrema. The extensions of the LED and ELED theories to systems of equations are also examined by considering several evolution processes, i.e. flux splitting methods. Higher-order dissipation schemes based on the LED or ELED principle combined with three flux splitting methods are applied to well-defined test problems that contain the essential physics of high speed unsteady flows : strong moving shocks, contact discontinuities and high expansion regions. The numerical results are carefully examined and the performance of each numerical scheme is assessed.

1 Introduction

Due to its complex physics which mainly comes from linear and non-linear wave interactions, the numerical computation of unsteady compressible flow presents a challenge which has enjoyed considerable attention. If viscous effects are neglected, the essential physics of high speed unsteady flows can be summarized as complex shock interactions, contact discontinuities and high expansion regions. The ultimate goal of modern shock capturing schemes would be the correct resolution of these structures, a high level of accuracy in a smooth flow and computational efficiency. Although the goal has proved to be quite elusive, most shock capturing schemes developed so far have been heavily concentrated on satisfying all or part of those requirements. Our present work is also directed towards this challenge. Over the past few decades, remarkable progress has been made in this area. FCT (Flux Corrected Transport)([1], [2]), TVD (Total Variation Diminishing)([3], [4]), MUSCL (Monotonic Upwind Schemes for Conservation Laws)([5], [6]), PPM (Piecewise Parabolic Method)([7]), ENO (Essentially Non-Oscillation)([9], [10], [11], [12]) and some Riemann solvers or flux splitting schemes ([13], [14], [15], [16], [17], [18]) would be the most noticeable breakthroughs. Gas-kinetic schemes have also been emerging as a very promising way to achieve the ultimate goal([19], [20], [21]). Most of those schemes can be largely categorized as

a) First-order schemes which describe the physical behavior of gas dynamic systems of equations, i.e., the Euler equations.

b) Higher-order schemes that satisfy a monotonicity constraint weakly or strongly. These schemes can be applied strictly to a scalar conservation law, while they are extended to systems of equations by combining with the schemes in the category of a).

An interesting exception for this categorization is a gas-kinetic approach([21]). Recently, Jameson has developed the theory of non-oscillatory shock capturing schemes in terms of the LED and ELED principles that belong to the category of b)([22], [23]). The LED principle satisfies the condition of Total Variation Diminishing (TVD) in one-dimensional cases, while it can be readily extended to multi-dimensional structured or unstructured grids without destroying the desired property, which is essentially a positivity condition. LED schemes have proved to be accurate and efficient in steady viscous and inviscid compressible flows ([22], [23],

* Research Assistant
†James S. McDonnell Distinguished University Professor of Aerospace Engineering, AIAA Fellow

Copyright ©1995 by the American Institute of Aeronautics and Astronautics, Inc. All rights reserved.

[26]). The LED principle can be satisfied by making the coefficients of the discrete approximation non-negative. This positivity condition allows us to examine the classical Jameson-Schmidt-Turkel (JST) scheme ([24]) from a different point of view, which leads to Symmetric or Upstream LImited Positive (SLIP or USLIP) formulations. To extend the LED and ELED principles to systems of equations, three different flux splitting methods which belong to the category of a) have been considered - characteristic splitting using Roe average, a newly formulated CUSP (Convective Upwind and Split Pressure) type flux splitting and HLL (Harten, Lax and Van Leer) flux splitting. In the present work, five flux limited dissipation schemes have been formulated by combining the LED and ELED principle with the three different flux splitting schemes. The resultant schemes have been applied to well-known one-dimensional and two-dimensional unsteady test problems and their performance has been carefully analyzed in terms of accuracy and robustness.

2 LED Schemes for Hyperbolic Conservation Laws

We start the theory of LED schemes by observing that

- The greatest value of TVD schemes would be the preservation of monotonicity.

- The direct extension of TVD schemes to the multi-dimensional case has proved to be quite restrictive due to the fact that any conservative TVD scheme in two-dimensional cases is at most first-order accurate([27]).

These indicate the necessity of developing a more flexible condition that can guarantee not only the preservation of monotonicity but also higher-order accuracy in a multi-dimensional scalar conservation law. This is achieved by controlling local extrema instead of measuring total variation. Therefore, corresponding mathematical tool is a local L_{inf} norm instead of L_1 norm.

As a model equation of fluid dynamics, we may consider the scalar hyperbolic conservation law of the form

$$\frac{\partial v}{\partial t} + \frac{\partial f}{\partial x} + \frac{\partial g}{\partial y} = 0. \tag{1}$$

By using a cell-centered finite volume technique, the semi-discrete form of eqn.(1) can be expressed as

$$\frac{dv_j}{dt} = \sum_{k \neq j} c_{jk}(v_k - v_j), \tag{2}$$

for the j-th cell. Suppose that the coefficients(c_{jk}) are all non-negative. Then the scheme is stable in L_∞ norm, but may still allow local extrema to increase or may create local extrema. Therefore, the coefficients c_{jk} need to be zero except in the neighborhood of j-th cell. From eqn.(2), if v_j is a local maximum, $v_k - v_j \leq 0$ so $\frac{dv_j}{dt} \leq 0$. If v_j is a local minimum, $v_k - v_j \geq 0$ so $\frac{dv_j}{dt} \geq 0$. So, it is an LED scheme. Monotonicity is preserved due to the LED property. Thus, positivity of the coefficients is a sufficient condition to satisfy the LED principle. A fully discrete LED scheme can be derived by controlling the time step. In the case of forward Euler time stepping, eqn.(2) becomes

$$v_j^{n+1} = v_j^n + \Delta t \sum_{k \neq j} c_{jk}(v_k^n - v_j^n).$$

And the time step which guarantees positive coefficients is

$$\Delta t \leq \frac{1}{\sum_{k \neq j} c_{jk}}.$$

The relation between LED and TVD can be examined by considering total variation. The total variation of v in the one-dimensional case is expressed as

$$\begin{aligned} TV(v) &= \int_{-\infty}^{+\infty} |\frac{dv}{dx}| dx \\ &\cong \sum_{j=-\infty}^{+\infty} |v_{j+1} - v_j|, \end{aligned}$$

or

$$TV(v) = 2(\sum maxima - \sum minima). \tag{3}$$

From eqn.(3), it is clear that an LED scheme is TVD. In two-dimensional case, the extended definition of total variation would be

$$TV(v) = \int_{-\infty}^{+\infty} \| \nabla v \| \, dxdy. \tag{4}$$

If we apply this criterion to grids which have 2 peaks and 1 ridge, we may find that eqn.(4) does not give the correct answer([22]). Therefore, the direct extension of the TVD condition to multi-dimensional problems may not control oscillatory modes properly. Note that the LED principle can still control these modes effectively.

3 Construction of Monotonic Higher Order Schemes

For the one-dimensional scalar conservation law

$$\frac{\partial v}{\partial t} + \frac{\partial f}{\partial x} = 0,$$

the semi-discrete approximation for the j-th cell is given by

$$\Delta x \frac{dv}{dt} + h_{j+\frac{1}{2}} - h_{j-\frac{1}{2}} = 0. \quad (5)$$

The numerical flux $h_{j+\frac{1}{2}}$ may be expressed as the sum of a central differencing flux and an appropriately defined diffusive flux,

$$\begin{aligned} h_{j+\frac{1}{2}} &= \frac{1}{2}(f_j + f_{j+1}) - d_{j+\frac{1}{2}} \\ &= \frac{1}{2}(f_j + f_{j+1}) - \alpha_{j+\frac{1}{2}} \Delta v_{j+\frac{1}{2}}, \end{aligned}$$

with $\Delta v_{j+\frac{1}{2}} = v_{j+1} - v_j$. The least diffusive first order numerical flux which satisfies the LED condition is the first order upwind flux([22]), i.e.

$$d_{j+\frac{1}{2}} = \frac{1}{2}|a_{j+\frac{1}{2}}|\Delta v_{j+\frac{1}{2}},$$

where $a_{j+\frac{1}{2}}$ is an approximation of the local wave speed by Roe average. In this sense, upwind biasing is a good approach to construct non-oscillatory schemes.

Since any first order scheme is unnecessarily diffusive except across discontinuities, higher-order non-oscillatory schemes can be derived by introducing anti-diffusive terms, i.e. a higher order interpolation procedure in designing the diffusive flux. A simple possible way is to use the third order anti-diffusive term

$$d_{j+\frac{1}{2}} = \alpha_{j+\frac{1}{2}}[\Delta v_{j+\frac{1}{2}} - \frac{1}{2}(\Delta v_{j+\frac{3}{2}} + \Delta v_{j-\frac{1}{2}})]. \quad (6)$$

This simple arithmetic average, of course, violates the positivity condition leading to oscillatory behavior around a shock wave. An early attempt to cure this problem by introducing adaptive pressure switches was the classical JST scheme ([24]).

$$d_{j+\frac{1}{2}} = \epsilon^{(2)}_{j+\frac{1}{2}} \Delta v_{j+\frac{1}{2}}$$

$$-\epsilon^{(4)}_{j+\frac{1}{2}}(\Delta v_{j+\frac{3}{2}} - 2\Delta v_{j+\frac{1}{2}} + \Delta v_{j-\frac{1}{2}}). \quad (7)$$

Here, $\epsilon^{(2)}$ and $\epsilon^{(4)}$ may be regarded as detectors of extrema or as limiters. The JST scheme combined with the multigrid acceleration technique is extremely efficient in steady state calculations([25]). In its original form, the JST scheme is not fully upwind in supersonic regions and does not satisfy the positivity condition strictly. Improved forms of the JST scheme can be constructed by imposing the LED or ELED condition.

Approach I : Local Extremum Diminishing

In eqn.(6), instead of using a simple arithmetic average of neighboring differences, we may modify this term into the limited flux form of $L(\Delta v_{j+\frac{3}{2}}, \Delta v_{j-\frac{1}{2}})$ so that the net diffusive flux can satisfy the positivity condition. In other words, we introduce a more systematic interpolation procedure which can recognize extrema and satisfy positivity. A detailed derivation on the condition of limited flux can be found in the paper [22]. $L(u, v)$ is a limited average that has the following properties.

P1. $L(u, v) = L(v, u)$
P2. $L(\alpha u, \alpha v) = \alpha L(u, v)$
P3. $L(u, u) = u$
P4. $L(u, v) = 0$ if u and v has an opposite sign, otherwise $L(u, v)$ has the same sign as u and v

Here, P1 and P2 are natural properties of an average. P3 is needed for the consistency of a numerical scheme. P4 is a crucial property to obtain positivity. A variety of limiters may be defined that meet the properties(P1-P4)([22], [30]). Now, the modified diffusive flux is

$$d_{j+\frac{1}{2}} = \alpha_{j+\frac{1}{2}}[\Delta v_{j+\frac{1}{2}} - L(\Delta v_{j+\frac{3}{2}}, \Delta v_{j-\frac{1}{2}})]. \quad (8)$$

Since this scheme limits the anti-diffusive flux in a symmetric manner and maintains positivity, it will be called a Symmetric Limited Positive(SLIP) scheme. A more general form of a SLIP scheme may be derived without violating the positivity condition

$$d_{j+\frac{1}{2}} = \alpha_{j+\frac{1}{2}} \Delta v_{j+\frac{1}{2}}$$

$$-L(\alpha_{j+\frac{3}{2}} \Delta v_{j+\frac{3}{2}}, \alpha_{j-\frac{1}{2}} \Delta v_{j-\frac{1}{2}}). \quad (9)$$

The diffusive flux reverts to first-order accuracy at extrema due to P4. Away from extrema, it recovers higher-order diffusion. Noting the fact that upwind biasing usually gives a less diffusive flux (recall that the least diffusive first order numerical flux which satisfies the LED condition is the first order upwind flux), an upstream version of the original SLIP scheme can be derived by considering wave motion in the anti-diffusive flux(8). The diffusive flux of the USLIP (Upstream Limited Positive) scheme is obtained by

$$d_{j+\frac{1}{2}} = \alpha_{j+\frac{1}{2}}[\Delta v_{j+\frac{1}{2}} - L(\Delta v_{j+\frac{1}{2}}, \Delta v_{j-\frac{1}{2}})] \quad (10)$$

if $a_{j+\frac{1}{2}} \geq 0$, or

$$d_{j+\frac{1}{2}} = \alpha_{j+\frac{1}{2}}[\Delta v_{j+\frac{1}{2}} - L(\Delta v_{j+\frac{3}{2}}, \Delta v_{j+\frac{1}{2}})]$$

if $a_{j+\frac{1}{2}} < 0$.

Approach II : Essentially Local Extremum Diminishing

LED limiters of Approach I turn off across discontinuities leading to a first-order diffusive flux of

$d_{j+\frac{1}{2}}$. This is enough to maintain a monotonic profile across shock waves or contact discontinuities. It is, however,unnecessarily diffusive at smooth extrema. In order to prevent this situation, we define $R(u,v)$ as

$$R(u,v) = \begin{cases} |\frac{u-v}{max(|u|+|v|,\epsilon\Delta x^r)}|^q & \text{if } u \neq 0 \text{ or } v \neq 0 \\ 0 & \text{if } u = v = 0 \end{cases},$$

where q, r are positive intergers and $\epsilon > 0$. Then $R(u,v) = 1$, if u and v have opposite signs and $|u| + |v| \geq \epsilon\Delta x^r$. Otherwise $R(u,v) < 1$. Now, we define a symmetric form of the ELED limiter as

$$\tilde{L}(\Delta u_{j+\frac{3}{2}}, \Delta u_{j-\frac{1}{2}}) = \frac{1}{2}D(\Delta u_{j+\frac{3}{2}}, \Delta u_{j-\frac{1}{2}})(\Delta u_{j+\frac{3}{2}} + \Delta u_{j-\frac{1}{2}}),$$

where

$$D(\Delta u_{j+\frac{3}{2}}, \Delta u_{j-\frac{1}{2}}) = 1 - R(\Delta u_{j+\frac{3}{2}}, \Delta u_{j-\frac{1}{2}})$$

$$= 1 - |\frac{\Delta u_{j+\frac{3}{2}} - \Delta u_{j-\frac{1}{2}}}{max(|\Delta u_{j+\frac{3}{2}}| + |\Delta u_{j-\frac{1}{2}}|, \epsilon\Delta x^r)}|^q .$$

An upstream version of the ELED limiter can also be obtained by replacing the anti-diffusive flux of eqn.(10) with $\tilde{L}(\Delta u_{j+\frac{1}{2}}, \Delta u_{j-\frac{1}{2}})$ and $\tilde{L}(\Delta u_{j+\frac{3}{2}}, \Delta u_{j+\frac{1}{2}})$.

If $|\Delta u_{j+\frac{3}{2}}| + |\Delta u_{j-\frac{1}{2}}|$ is less than $\epsilon\Delta x^r$, which usually occurs at smooth extrema, $\tilde{L}(\Delta u_{j+\frac{3}{2}}, \Delta u_{j-\frac{1}{2}})$ is still active giving a higher-order diffusive flux. This can be shown more quantitatively by rearranging the diffusive flux as

$$\tilde{d}_{j+\frac{1}{2}} = \alpha_{j+\frac{1}{2}}[\Delta v_{j+\frac{1}{2}} - \tilde{L}(\Delta v_{j+\frac{3}{2}}, \Delta v_{j-\frac{1}{2}})]$$

$$= \frac{\alpha_{j+\frac{1}{2}}}{2}[(2\Delta v_{j+\frac{1}{2}} - \Delta v_{j+\frac{3}{2}} - \Delta v_{j-\frac{1}{2}})$$

$$-(\Delta v_{j+\frac{3}{2}} + \Delta v_{j-\frac{1}{2}})R(\Delta v_{j+\frac{3}{2}}, \Delta v_{j-\frac{1}{2}})]. \quad (11)$$

The first term of $\tilde{d}_{j+\frac{1}{2}}$ is $O(\Delta x^3)$ and the second term is $O(\Delta x^{(2-r)q})$ in smooth regions including smooth extrema, so the order of total flux is $O(\Delta x^{(2-r)q})$. Similarly, from eqn.(11) and eqn.(5) one can show that

$$\frac{dv_j}{dt} = \begin{cases} \leq \frac{1}{2}(\alpha_{j+\frac{1}{2}} + \alpha_{j-\frac{1}{2}})\epsilon\Delta x^{r-1} & v_j = \text{a max} \\ \geq -\frac{1}{2}(\alpha_{j+\frac{1}{2}} + \alpha_{j-\frac{1}{2}})\epsilon\Delta x^{r-1} & v_j = \text{a min} \end{cases}, \quad (12)$$

Thus, if $0 < r < 2$ and $q > \frac{2}{2-r}$, $d_{j+\frac{1}{2}} = O(\Delta x^2)$ at smooth extrema. From eqn.(12), if $r > 1$, $\frac{dv_j}{dt} \rightarrow \pm 0$ as $\Delta x \rightarrow 0$ giving essentially local extremum diminishing(ELED). Therefore, the proper range of r is $1 < r < 2$.

If $|\Delta u_{j+\frac{3}{2}}| + |\Delta u_{j-\frac{1}{2}}|$ is greater than $\epsilon\Delta x^r$, $\tilde{L}(\Delta u_{j+\frac{3}{2}}, \Delta u_{j-\frac{1}{2}})$ reduces to $L(\Delta u_{j+\frac{3}{2}}, \Delta u_{j-\frac{1}{2}})$ and for $q = 1$ or 2, $L(\Delta u_{j+\frac{3}{2}}, \Delta u_{j-\frac{1}{2}})$ becomes a minmod or Van Leer limiter, respectively. One can get a more compressive limiter by increasing the exponent q. From the definition of the ELED limiter, one can see $\tilde{L}(\Delta u_{j+\frac{3}{2}}, \Delta u_{j-\frac{1}{2}}) \rightarrow \frac{1}{2}(\Delta u_{j+\frac{3}{2}} + \Delta u_{j-\frac{1}{2}})$ as $q \rightarrow \infty$ leading to the simple arithmetic average of eqn.(6). By increasing q one can improve the accuracy of a scheme except in the neighborhood of stiff extrema. It should be mentioned here that the ELED approach shares the same spirit with the ENO interpolation of Harten *et al.*([10]) in the sense that both schemes try to circumvent the side effect of a monotonic limiter by allowing local extrema (or total variation in ENO interpolation) to increase based on some power of the grid size. This can be seen by observing that in ENO interpolation, we can say

$$TV(v_j^{n+1}) \leq TV(v_j^n) + O(\Delta x^r),$$

for some $r > 0$, if there are at least $r + 1$ smooth points between local extrema.

4 Extension to Systems of Equations

So far, we have derived schemes for scalar conservation laws from LED and ELED approaches, while the governing equations of fluid dynamics, for example the Euler equations, are systems of equations. The extension of numerical schemes to systems of equations usually requires the knowledge of the dynamic behavior of the governing equations under certain initial conditions. It is this field where the physical understanding of the fluid dynamics is decisive in designing numerical schemes. Numerical schemes of the Euler equations are usually expressed as first-order schemes which are too diffusive for most aerodynamic computations. Higher-order schemes can be obtained by coupling first-order schemes with the higher-order interpolation procedure described in section 3. Therefore, both aspects should be considered when we judge the quality of numerical schemes. In the present work, we have considered three different flux splitting methods - characteristic splitting with Roe average([14]), a newly formulated CUSP type splitting([23]) and HLL flux splitting([15]). Gas-kinetic schemes combined with LED limiters have also proved to be quite accurate and robust. Readers who are interested in this approach should refer to the papers [20], [21]. Assuming that readers are familiar with the first method, we start from the second method.

HLL Flux Splitting

Consider the one-dimensional Euler equations of the form

$$\frac{\partial v}{\partial t} + \frac{\partial f}{\partial x} = 0$$

with

$$v = (\rho, \rho u, \rho E)^T, f = (\rho u, \rho u^2 + p, \rho u H)^T,$$

where ρ is the density, u is the velocity, E is the total energy, p is the pressure and H is the total enthalpy. The numerical flux of HLL splitting at the cell interface can be expressed as

$$h_{j+\frac{1}{2}} = \frac{1}{2}(f_j + f_{j+1}) - \frac{1}{2}B_{j+\frac{1}{2}}\Delta v_{j+\frac{1}{2}}, \qquad (13)$$

where $B_{j+\frac{1}{2}} = \frac{b^r_{j+\frac{1}{2}} + b^r_{j+\frac{1}{2}}}{b^r_{j+\frac{1}{2}} - b^l_{j+\frac{1}{2}}} A_{j+\frac{1}{2}} - 2\frac{b^r_{j+\frac{1}{2}} b^l_{j+\frac{1}{2}}}{b^r_{j+\frac{1}{2}} - b^l_{j+\frac{1}{2}}} I.$

b^r, b^l are the approximate wave speeds and $A_{j+\frac{1}{2}}$ is the Jacobian matrix constructed by Roe average. Compared to the characteristic splitting, HLL splitting captures only two non-linear waves$(u+c, u-c)$. Therefore, one may expect the smearing of a contact discontinuity, especially in a multi-dimensional flow. The estimation of the wave speeds is crucial. For example, if we simply use $b^r = u + c$ and $b^l = u - c$, the eigenvalues of $B_{j+\frac{1}{2}}$ are $c, u+c$ and $c-u$. In the present work, we have used Einfeldt's estimation of b^r, b^l. See [28] for the details.

$$b^r_{j+\frac{1}{2}} = Max(0, \hat{u}_{j+\frac{1}{2}} + \hat{c}_{j+\frac{1}{2}}, u_{j+1} + c_{j+1}),$$

$$b^l_{j+\frac{1}{2}} = Min(0, \hat{u}_{j+\frac{1}{2}} - \hat{c}_{j+\frac{1}{2}}, u_j - c_j),$$

where $\hat{u} \pm \hat{c}$ are the wave speeds calculated by the Roe average.

The implementation of LED or ELED is rather straightforward. From eqn.(12),

$$d_{j+\frac{1}{2}} = \tfrac{1}{2}B_{j+\frac{1}{2}}\Delta v_{j+\frac{1}{2}}$$

$$= \tfrac{1}{2}(T^{-1}\tilde{\Lambda}T)_{j+\frac{1}{2}}\Delta v_{j+\frac{1}{2}}, \qquad (14)$$

where $\tilde{\Lambda} = \frac{b^r+b^l}{b^r-b^l}\Lambda - \frac{2b^r b^l}{b^r-b^l}I$. Λ is a diagonal matrix containing the Roe averaged eigenvalues and T is the matrix of eigenvectors. The symmetric flux limited form of eqn.(13) is given by

$$d_{j+\frac{1}{2}} = \frac{1}{2}(T^{-1}\tilde{\Lambda})_{j+\frac{1}{2}}[\Delta w_{j+\frac{1}{2}} - L^*(\Delta w_{j+\frac{3}{2}}, \Delta w_{j-\frac{1}{2}})],$$

or

$$d_{j+\frac{1}{2}} = \tfrac{1}{2}T^{-1}_{j+\frac{1}{2}}[\tilde{\Lambda}_{j+\frac{1}{2}}\Delta w_{j+\frac{1}{2}}$$

$$-L^*(\tilde{\Lambda}_{j+\frac{3}{2}}\Delta w_{j+\frac{3}{2}}, \tilde{\Lambda}_{j-\frac{1}{2}}\Delta w_{j-\frac{1}{2}})],$$

where $\Delta w = T\Delta v$ and L^* is L or $\tilde{L}$. Note that we have applied the limiting process to characteristic variables. Following the MUSCL approach, the same limiting process can be applied to conservative variables. However, we prefer the first technique due to the fact that characteristic variables are usually smoother than conservative variables. The same limiting process has been applied to the characteristic splitting method.

CUSP Type Flux Splitting

A disadvantage of the HLL flux splitting is that its performance is very dependent on the estimation of wave speeds. A more general form of flux splitting is obtained by observing that the diffusive flux of eqn.(13) can be expressed as

$$d_{j+\frac{1}{2}} = \tfrac{1}{2}B_{j+\frac{1}{2}}\Delta v_{j+\frac{1}{2}} = \tfrac{1}{2}(\frac{b^r_{j+\frac{1}{2}} + b^l_{j+\frac{1}{2}}}{b^r_{j+\frac{1}{2}} - b^l_{j+\frac{1}{2}}})\Delta f_{j+\frac{1}{2}}$$

$$+\tfrac{1}{2}(-\frac{2b^r_{j+\frac{1}{2}} b^l_{j+\frac{1}{2}}}{b^r_{j+\frac{1}{2}} - b^l_{j+\frac{1}{2}}})\Delta v_{j+\frac{1}{2}}.$$

To avoid the estimation of wave speeds, blending functions are introduced to get

$$d_{j+\frac{1}{2}} = \frac{1}{2}[\alpha^* c\Delta v_{j+\frac{1}{2}} + \beta\Delta f_{j+\frac{1}{2}}], \qquad (15)$$

where α^*, β are blending functions and c is the speed of sound. By introducing the CUSP splitting, the flux vector is decomposed as

$$f = u\begin{pmatrix}\rho\\ \rho u\\ \rho E\end{pmatrix} + \begin{pmatrix}0\\ p\\ pu\end{pmatrix} \equiv uv + f_p \qquad (16)$$

and

$$\Delta f_{j+\frac{1}{2}} = \bar{u}\Delta v_{j+\frac{1}{2}} + \bar{v}\Delta u_{j+\frac{1}{2}} + \Delta f_{p_{j+\frac{1}{2}}}, \qquad (17)$$

where $\bar{u} = \frac{1}{2}(u_{j+1} + u_j), \bar{v} = \frac{1}{2}(v_{j+1} + v_j)$. From eqn.(14) and (16), we get

$$d_{j+\frac{1}{2}} = \frac{\alpha c}{2}\Delta v_{j+\frac{1}{2}} + \frac{\beta}{2}(\bar{v}\Delta u_{j+\frac{1}{2}} + \Delta f_{p_{j+\frac{1}{2}}}), \qquad (18)$$

with $\alpha c \equiv \alpha^* c + \beta\bar{u}$. As an alternative way, we can introduce a modified state vector $w_h = (\rho, \rho u, \rho H)^T$ in eqn.(14), (15), (16) and (17) instead of v to make total enthalpy constant in steady state flows. In this case, f_p is $(0, p, 0)^T$. It follows that from eqn.(14), full upwinding is achieved if $\alpha^* = 0$, $\beta = sign(M)$ requiring that $\alpha = |M|$, $\beta = sign(M)$ in supersonic regions. In subsonic regions, α, β must also be formulated such that they behave symmetrically with respect to a stagnation point. A safe choice for α is

$$\alpha = \begin{cases} |M| & \text{if } |M| > \epsilon \\ \frac{1}{2}(\epsilon + \frac{|M|^2}{\epsilon}) & \text{if } |M| \le \epsilon \end{cases},$$

and β is

$$\beta = \begin{cases} Max(0, 2M-1) & \text{if } 0 \le M \le 1, \\ Min(0, 2M+1) & \text{if } -1 \le M \le 0 \\ sign(M) & \text{if } |M| \ge 1 \end{cases},$$

With this choice of α and β, Jameson has shown([23]) that the scheme allows a discrete stationary shock with a single interior point. We can see the low diffusive character of this scheme from Fig.1. If the CUSP scheme is directly combined with HLL splitting, it is very diffusive. A higher-order CUSP scheme can be obtained by MUSCL type interpolation. Left and right state values of a cell interface are interpolated by using a LED or ELED limiter as follows,

$$q^L = q_j + \frac{1}{2}L^*(\Delta q_{j+\frac{3}{2}}, \Delta q_{j-\frac{1}{2}}),$$
$$q^R = q_{j+1} - \frac{1}{2}L^*(\Delta q_{j+\frac{3}{2}}, \Delta q_{j-\frac{1}{2}}),$$

where q is v or w_h. The interpolated states (q^L, q^R) are used to get the higher order diffusive flux of eqn.(17).

5 Numerical Results

A family of flux limited schemes can be obtained by combining symmetric or upstream versions of LED or ELED limiters with three flux splittings. In the present work, Symmetric LED and ELED limiters are chosen to maintain robustness of numerical schemes. Five schemes (Csplit-LED, Csplit-ELED, CUSP-ELED, HLL-LED, HLL-ELED) are formulated and tested. See Table 1. The role of monotonic limiters is generally known as problem-dependent. For example, the Superbee limiter gives an accurate result in a discontinuous region, while it produces a clipping of extrema in smooth regions due to over-compression. On the other hand, the Minmod limiter does not clip smooth extrema but is diffusive especially in a discontinuous region. It would be rather undesirable to change limiters or coefficients of limiters for each test case. In the present work, the symmetric version of the α-mean limiter is chosen as a LED limiter. This is defined by

$$L(\Delta v_{j+\frac{3}{2}}, \Delta v_{j-\frac{1}{2}}) = S(\Delta v_{j+\frac{3}{2}}, \Delta v_{j-\frac{1}{2}}) *$$

$$Min(\frac{|\Delta v_{j+\frac{3}{2}} + \Delta v_{j-\frac{1}{2}}|}{2}, \alpha\Delta v_{j+\frac{3}{2}}, \alpha\Delta v_{j-\frac{1}{2}}),$$

with $S(\Delta v_{j+\frac{3}{2}}, \Delta v_{j-\frac{1}{2}}) = \frac{1}{2}[sign(\Delta v_{j+\frac{3}{2}}) + sign(\Delta v_{j-\frac{1}{2}})]$. α is fixed to 2. For this value, it is identical to the MUSCL limiter. For the same reason, the exponent q in the ELED limiter(11) is fixed to 3 for all test cases. The Superbee limiter is used to compensate for the diffusive character of HLL splitting. A conventional 4th-order Runge-Kutta time integration is used to obtain time accuracy.

The first test case is a one-dimensional blast wave problem proposed by Woodward and Colella([8]). By the collision of two blast waves, a new contact discontinuity emerges at the center. Two shocks and three contact discontinuities must be resolved with an expansion region in the middle. The number of grid cells is 400 and the results are compared with an 800 cell calculation by characteristic splitting with an upstream version of the LED limiter(eqn.(10)). Fig.2 - Fig.6 are density and pressure profiles at $t = 0.038$. Every scheme captures the shock waves within two or three interior points without spurious oscillation. In contact discontinuities or expansion regions, the CUSP-ELED scheme gives slightly more diffusive results compared to the other schemes. The Csplit-ELED scheme produces a slightly higher peak and gives better results in every region than the Csplit-LED scheme proving the accuracy of the ELED approach. The HLL-LED and HLL-ELED schemes also give very good results partly due to the compressive property of the Superbee limiter.

The second test case concerns flow over a forward facing step. Freestream quantities with $M_\infty = 3.0$ are fixed at the inlet, while at the exit, every variable is extrapolated from the inside. On the upper and lower boundary, reflecting boundary conditions have been applied. To see the behavior of the expansion fan and the presence of a Mach stem on top of the step, no special treatment has been applied to the step corner. Thirty equally spaced contours divided by extrema values are given. Although a grid refinement study has been done with three different grid sizes($\Delta x = \Delta y = \frac{1}{20}, \frac{1}{40}, \frac{1}{80}$), only the results of fine grid calculation($\Delta x = \Delta y = \frac{1}{80}$) is presented for the sake of brevity. The unit length is the vertical height of computational domain. Fig.7 - Fig.11 are the density and entropy contours at $t = 4.0$. The Csplit-LED and Csplit-ELED schemes resolve the shock waves more sharply than the other schemes and the resolution of a contact discontinuity is very good. This advantage, however, seems to be counterbalanced by the presence of a very stiff expansion fan around the step corner. Some instability of normal shocks has also been observed in the transient shock motions on the upper and lower boundary. This problem will be discussed later. In the case of the CUSP-ELED scheme, the contact discontinuity is somewhat diffused compared to the Csplit-LED or Csplit-ELED schemes while the expansion fan around the corner is more rounded. The oblique shock reflected from the top of the forward step produces the noticeable Mach stem. This Mach stem has not been observed in the case of the Csplit-LED and Csplit-ELED schemes. The HLL-LED and HLL-ELED schemes show qualitatively the same results but the resolution of the contact discontinuity is better than the CUSP-ELED scheme. To see the resolution of all discontinuities(a normal shock, an oblique shock and a contact discontinuity), density

distributions along a horizontal line at a distance of 14 cells from the top and along a vertical line 14 cells to the right of the step corner are compared(Fig.12). As in the first test case, all schemes capture the normal shock within two points. Oblique shocks and the contact discontinuity are captured within four or five points. The location of the normal shock or oblique shocks or the presence of the Mach stem are slightly different for each flux splitting method indicating the importance of the proper amount of artificial dissipation in high speed unsteady flow computations.

It is generally known that schemes based on the characteristic splitting by Roe average can produce the carbuncle phenomenon in steady or near-steady flows with a slowly moving shock. According to the present computations, however, it can also happen in high speed unsteady flows with strong moving shocks if the shock is aligned to the grid. This phenomenon is aggravated as the number of cells increases. Recently, Quirk investigated some flaws of Godunov type schemes including the carbuncle phenomenon of the Roe scheme in a steady blunt body calculation ([31]). The following Mach reflection of the strong shock problem also confirms a somewhat dangerous behavior of characteristic splitting schemes using Roe average. A shock wave with $M_s = 10.0$ is located at the entrance of a 60 degree wedge and is propagated along the wedge. Fig.13 shows the development of an instability in the normal shock with $\Delta x = \Delta y = \frac{1}{120}$. Initially a slight instability is developed at the lower part of the normal shock. As the shock moves forward, the instability is magnified leading to a completely disrupted shock structure. Note that this happens in a first-order scheme with an entropy fix, not to mention of higher-order schemes(Csplit-LED, Csplit-ELED). This phenomenon, however, can be cured by increasing the artificial dissipation related to an entropy fix(Fig.14 - Fig.15). According to our experience, the amount of artificial dissipation seems to be dependent on several factors such as free stream conditions, geometry and grid distribution. The CUSP-ELED, HLL-LED and HLL-ELED schemes have not shown any similar behavior in grid refinement study($\Delta x = \Delta y = \frac{1}{30}, \frac{1}{60}, \frac{1}{120}$). See Fig.16 - Fig.18 for the case of $\Delta x = \Delta y = \frac{1}{60}$. The resolution of contact discontinuity emerged from the triple point is best in the cases of Csplit-LED, Csplit-ELED schemes as in the forward facing step problem.

Finally, we present a supersonic expansion problem with the HLL-LED and HLL-ELED schemes. Initially, a diaphragm located at the center with two different states of $(\rho_l,\ \rho u_l,\ \rho v_l,\ \rho E_l) = (1,-2,0,3)$ and $(\rho_r,\ \rho u_r,\ \rho v_r,\ \rho E_r) = (1,2,0,3)$ is ruptured to produce a very high expansion region in the center. This is the case where standard Roe type linearization fails due to the low density and low total energy developed in the center([29]). Fig.19 - Fig.20 show the density, pressure, velocity and energy distribution of the HLL, HLL-LED and HLL-ELED schemes at $t = 0.1$ with 100 cells. Compared with the exact solutions, we can see that the HLL-LED and HLL-ELED schemes improve the accuracy of HLL flux splitting greatly while keeping the robustness of the original first-order scheme.

6 Conclusions and Recommendations

In the present work, we have presented higher-order flux limited dissipation schemes for high speed unsteady flows using the LED and ELED approaches. We have examined the accuracy and robustness of each scheme by four unsteady test cases which contain the essential physics of high speed unsteady flows. The Csplit-LED or Csplit-ELED schemes capture shock waves and contact discontinuities very well while they show some undesirable properties such as a stiff expansion fan or the unsteady carbuncle phenomenon. Though the resolution of contact discontinuities are not so good as the Csplit-LED or Csplit-ELED schemes, the CUSP-ELED, HLL-LED and HLL-ELED schemes resolve shock waves crisply and prove to be quite robust.

All numerical results indicate that flux limited schemes based on the LED or ELED interpolation improve the accuracy greatly while maintaining the efficiency and robustness of original first-order schemes. Another point is that most properties of higher-order schemes are dependent on those of first-order schemes. This indicates that the development of a numerical scheme which faithfully describes the dynamic behavior of the Euler or Navier-Stokes equations is very important and much research should be done in this area. In designing such schemes, real physical aspects of fluid dynamics should be implemented as much as possible.

7 Acknowledgements

The research in this paper is partially supported by Grant URI/AFOSR F49620-93-1-0427. The first author thanks Prof. L. Martinelli for a helpful suggestion.

References

[1] J.P. Boris and D.L. Book,"Flux corrected transport, 1 SHASTA, a fluid transport algorithm that works," J. Comp. Phys., Vol.11, p38, 1973.

[2] S.T. Zalesak,"Fully Multidimensional Flux-Corrected Transport Algorithms for Fluids," J. Comp. Phys., Vol.31, p335, 1979.

[3] A. Harten,"High resolution schemes for hyperbolic conservation laws," J. Comp. Phys. Vol.49, p357, 1983.

[4] H.C. Yee,"Construction of Explicit and Implicit Symmetric TVD Schemes and Their Applications," J. Comp. Phys. Vol.68, p.151, 1983.

[5] B. Van Leer,"Towards the ultimate conservative difference scheme. IV, A New Approach to Numerical Convection," J. Comp. Phys., Vol.23, p276, 1977.

[6] B. Van Leer,"Towards the ultimate conservative difference scheme. V, A Second Order sequel to Godunov's Method," J. Comp. Phys., Vol.32, p101, 1979.

[7] P. Colella and P. Woodward,"The Piecewise Parabolic Method(PPM) for Gas-Dynamical Simulations," J. Comp. Phys., Vol.54, p174, 1984.

[8] P. Woodward and P. Colella,"The numerical simulation of two-dimensional fluid flow with strong shocks," J. Comp. Phys., Vol.54, p115, 1984.

[9] A. Harten and S. Osher,"Uniformly Higher-Order Accurate Essentially Non-Oscillatory Schemes I," SIAM J. Num. Anal., Vol.25, p294, 1988.

[10] A. Harten, B. Engquist, S. Osher and S. Chakravarthy,"Uniformly Higher-Order Accurate Essentially Non-Oscillatory Schemes III," J. Comp. Phys., Vol.71, p231, 1987.

[11] C.W. Shu and S. Osher,"Efficient Implementation of Essentially Non-Oscillatory Shock-Capturing Schemes," J. Comp. Phys., Vol.77, p439, 1988.

[12] C.W. Shu and S. Osher,"Efficient Implementation of Essentially Non-Oscillatory Shock-Capturing Schemes, II" J. Comp. Phys., Vol.82, p32, 1989.

[13] S.K. Godunov,"A Difference Scheme for the Numerical Computation of Discontinuous Solutions of Hydrodynamic Equations," Math. Sbornik, vol.47, p271, 1959.

[14] P.L. Roe,"Approximate Riemann solvers, parameter vectors, and difference schemes," J. Comp. Phys., Vol.43, p357, 1981.

[15] A. Harten, P.D. Lax, and B. Van Leer,"On upstream differencing and Godunov-type schemes for hyperbolic conservation laws," SIAM Rev., Vol.25, p35, 1983.

[16] B. Enquist and S. Osher,"Stable and Entropy Satisfying Approximations for Transonic Flow Calculations," Math. Comp., Vol.34, p45, 1980.

[17] M-S. Liou and C.J. Steffen,"A new flux splitting scheme," J. Comp. Phys., Vol.107, p23, 1993.

[18] J.L. Steger and R.F. Warming,"Flux vector splitting of the inviscid gas dynamics equations with applications to finite difference methods," J. Comp. Phys., Vol.40, p263, 1981.

[19] K. Xu and K.H. Predergast,"Numerical Navier-Stokes Solutions from Gas-Kinetic Theory," J. Comp. Phys., Vol.114, p9, 1994.

[20] K. Xu, L. Martinelli and A. Jameson,"Gas-Kinetic Finite Volume Methods, Flux-Vector Splitting and Artificial Diffusion," accepted for publication in J. Comp. Phys., Feb. 1995.

[21] C.A. Kim, K. Xu, A. Martinelli and A. Jameson,"The Gas-Kinetic BGK Scheme for Computational Gas Dynamics Applied to Advection Equations,", submitted to Int. J. Num. Met. in Fluids, Mar. 1995.

[22] A. Jameson,"Analysis and Design of Numerical Schemes for Gas Dynamics 1. Artificial Diffusion, Upwind Biasing, Limiters and Their Effect on Accuracy and Multigrid convergence,", accepted for publication in Int. J. Comp. Flu. Dyna., Feb. 1995.

[23] A. Jameson,"Analysis and Design of Numerical Schemes for Gas Dynamics 2. Artificial Diffusion and Discrete Shock Structure,", accepted for pubication in Int. J. Comp. Flu. Dyna., Feb. 1995.

[24] A. Jameson, W. Schmidt and E. Turkel,"Numerical Solution of Euler equation by finite volume methods with Runge-Kutta time stepping schemes," AIAA paper 81-1259, Jan. 1981.

[25] A.Jameson,"Multigrid algorithms for compressible flow calculations," Lecture Notes in Mathematics, Vol.1228, pp.166-201. Proceedings of the 2nd European Conference on Multigrid Methods, Colobne, 1985, Springer-Verlag, 1986.

[26] S. Tatsumi, L. Martinelli and A. Jameson,"Design, implementation, and validation of flux limited schemes for the solution of the compressible Navier-Stokes equations," AIAA J., Vol.33, p252, 1995.

[27] J.B. Goodman and J. LeVeque,"On the Accuracy of Stable Schemes for 2D Scalar Conservation Laws,", Math. Comp., Vol.45, No.171, p15, 1985.

[28] B. Einfeldt,"On Godunov-type methods for gas dynamics," SIAM J. Num. Anal., Vol.25, p294, 1988.

[29] B. Einfeldt, C.D. Munz, P.L. Roe and B. Sjögreen "On Godunov-type Methods Near Low Densities," J. Comp. Phys., Vol.92, p273, 1991.

[30] P.K. Sweby,"High Resolution Schemes using Flux Limiters for Hyperbolic Conservation Laws," SIAM J. Num. Anal., Vol.21, p995, 1984.

[31] J.J. Quirk,"A contribution to the great Riemann solver debate," Int. J. Num. Met. in Fluids., Vol.18, p555, 1994.

[32] R.C. Swanson and E. Turkel,"On central-difference and upwind schemes," J. Comp. Phys., Vol.101, p297, 1992.

[33] P.D. Lax,"Hyperbolic systems of conservation laws," SIAM regional series on Appl. Math., 1973.

	Characteristic	CUSP	HLL
Symmetric LED	Csplit-LED		HLL-LED
Symmetric ELED	Csplit-ELED	CUSP-ELED	HLL-ELED

Table 1: Flux Limited Dissipation Schemes

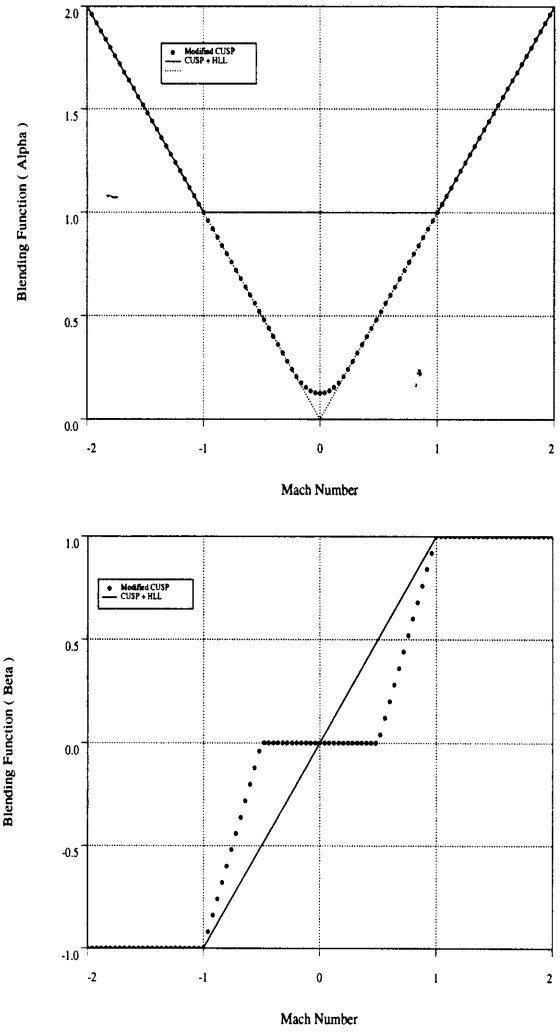

Figure 1: Comparison of Blending Functions : CUSP+HLL(—), Modified CUSP(...)

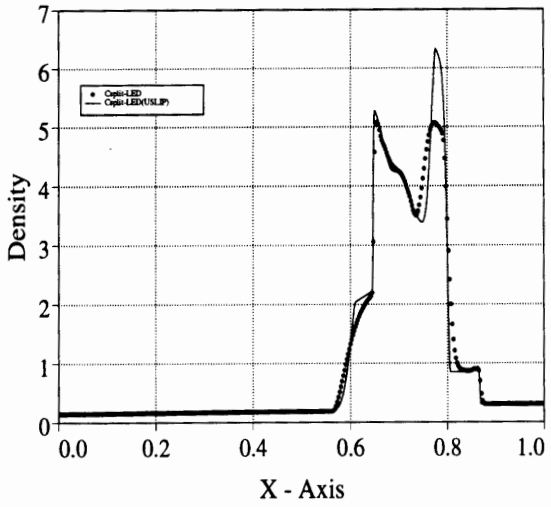

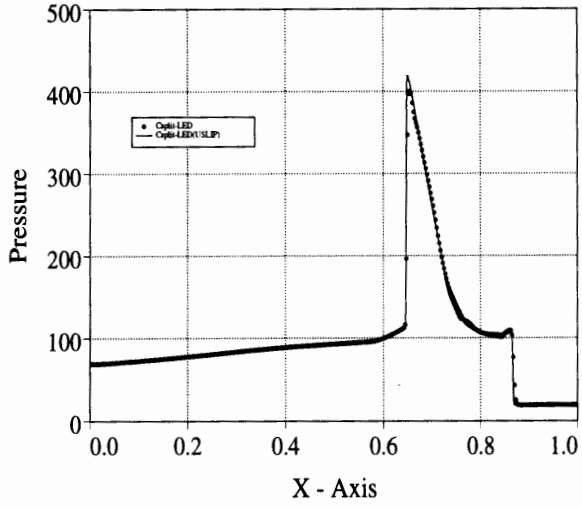

Figure 2: Blast Wave (Csplit-LED(...) : Csplit-USLIP(—), Density and Pressure)

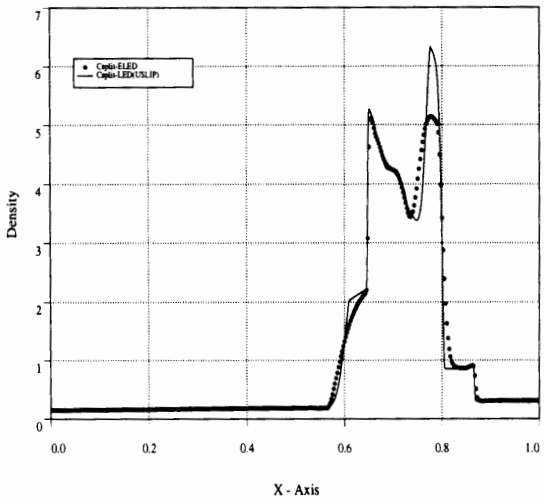

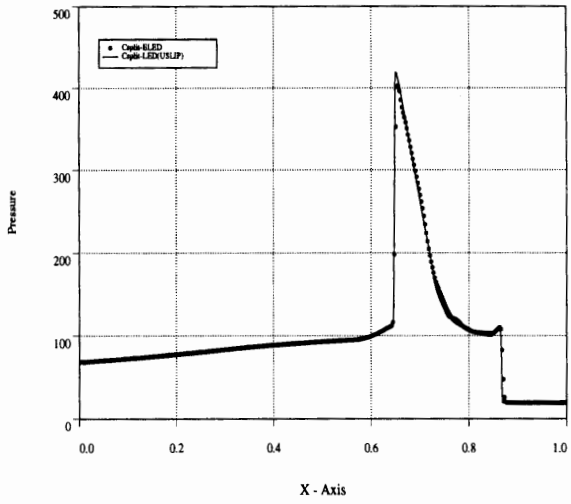

Figure 3: Blast Wave (Csplit-ELED(...) : Csplit-USLIP(—), Density and Pressure)

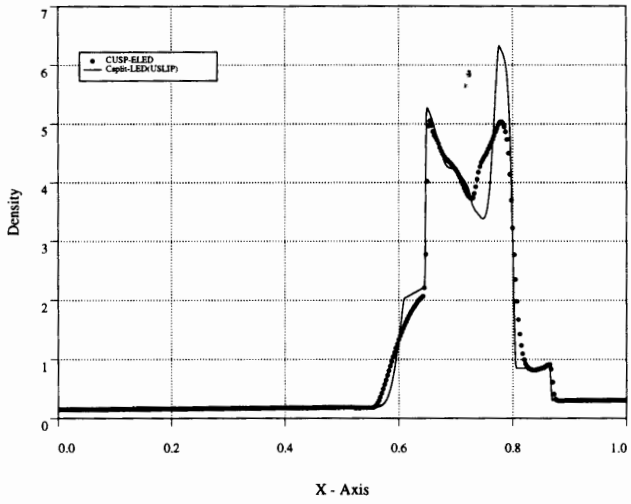

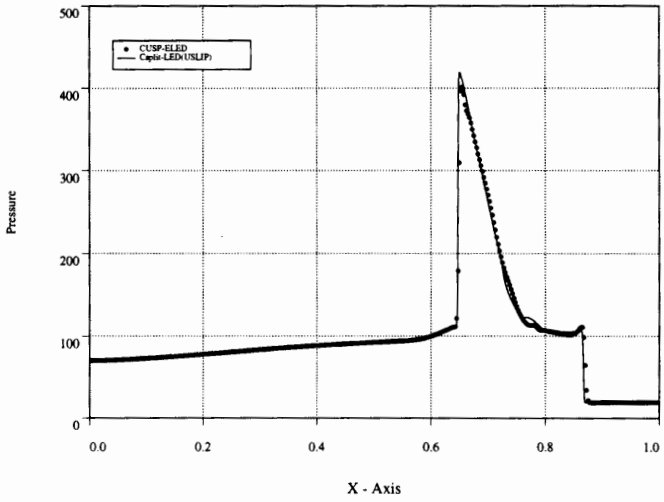

Figure 4: Blast Wave (CUSP-ELED(...) : Csplit-USLIP(—), Density and Pressure)

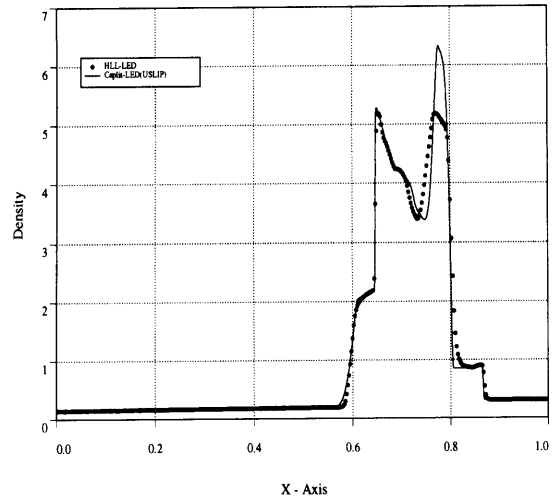

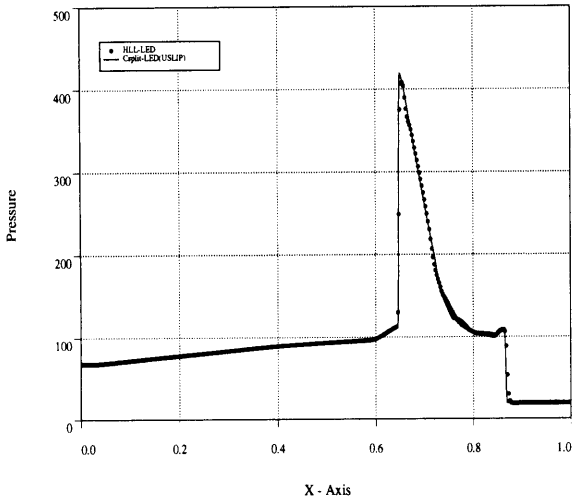

Figure 5: Blast Wave (HLL-LED(...) : Csplit-USLIP(—), Density and Pressure)

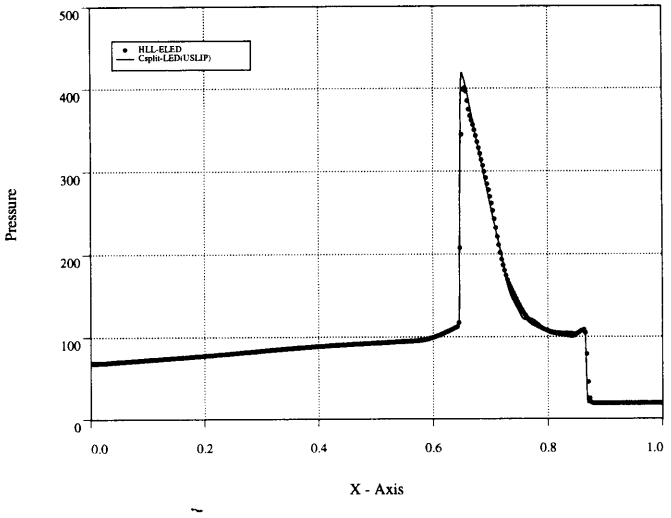

Figure 6: Blast Wave (HLL-ELED(...) : Csplit-USLIP(—), Density and Pressure)

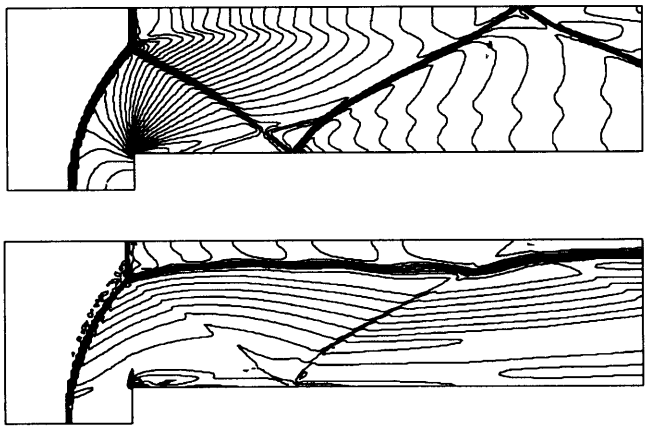

Figure 7: Forwave Facing Step with M = 3.0 (Csplit-LED, Density and Entropy)

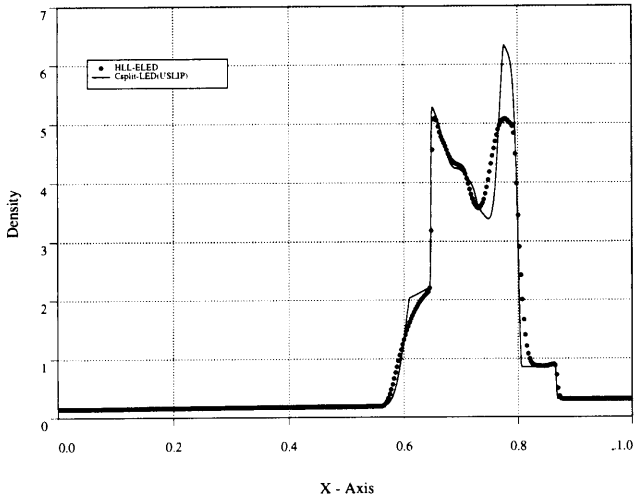

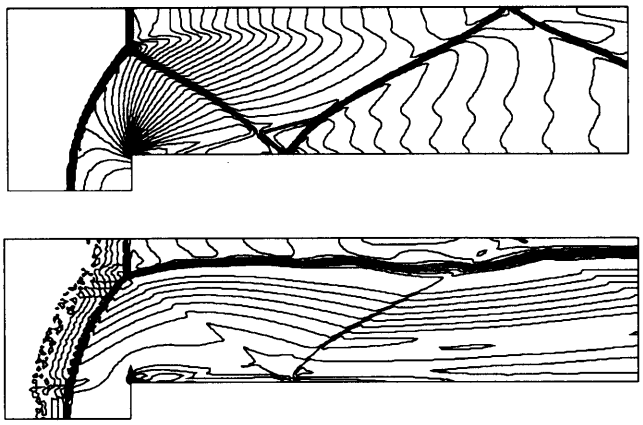

Figure 8: Forwave Facing Step with M = 3.0 (Csplit-ELED, Density and Entropy)

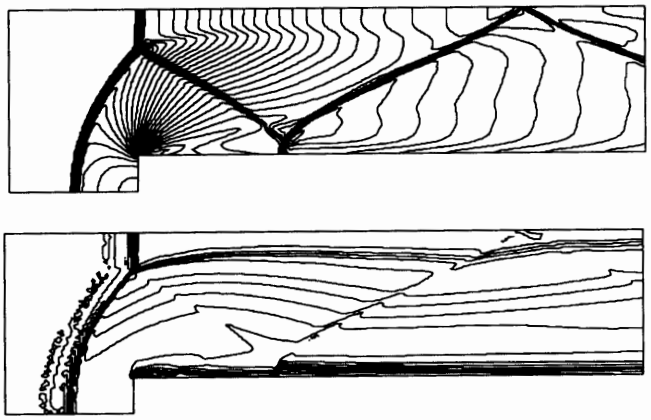

Figure 9: Forwave Facing Step with M = 3.0 (CUSP-ELED, Density and Entropy)

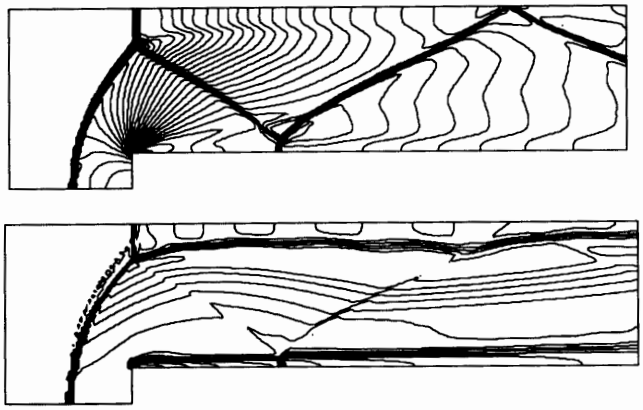

Figure 10: Forwave Facing Step with M = 3.0 (HLL-LED, Density and Entropy)

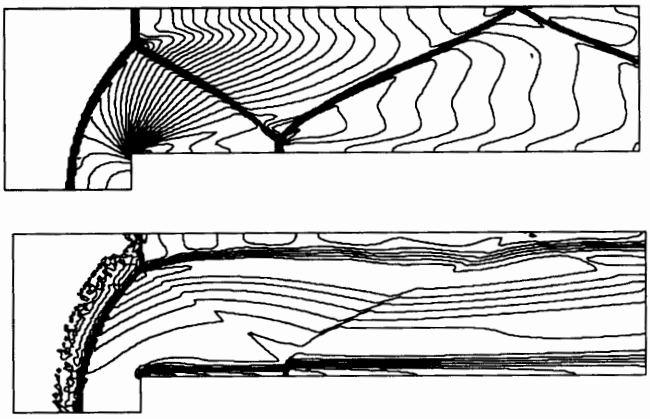

Figure 11: Forwave Facing Step with M = 3.0 (HLL-ELED, Density and Entropy)

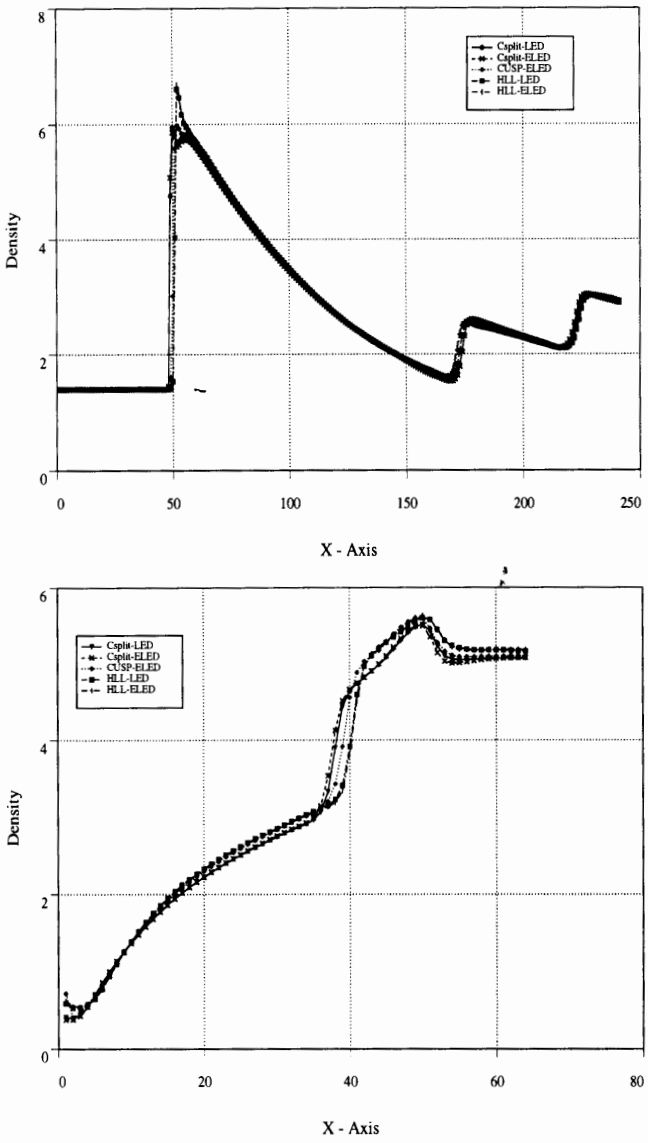

Figure 12: Density Distribution along Horizontal and Vertical Line

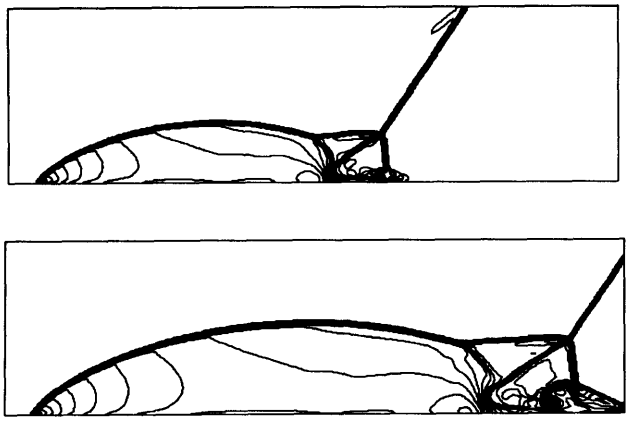

Figure 13: Development of the Unsteady Carbuncle Phenomenon (Characteristic Splitting, Density)

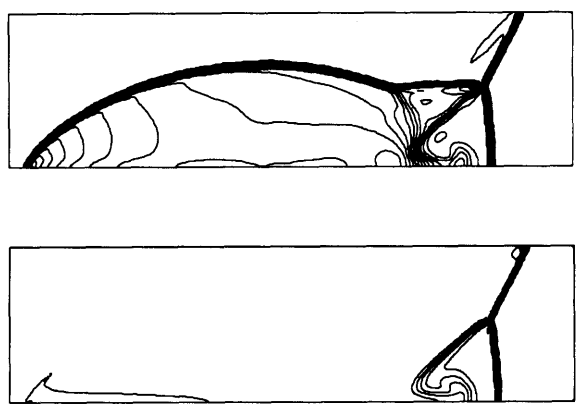

Figure 14: Double Mach Reflection (Csplit-LED, Density and Entropy)

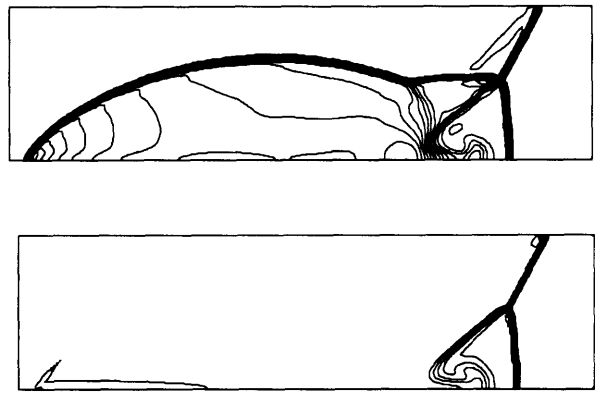

Figure 15: Double Mach Reflection (Csplit-ELED, Density and Entropy)

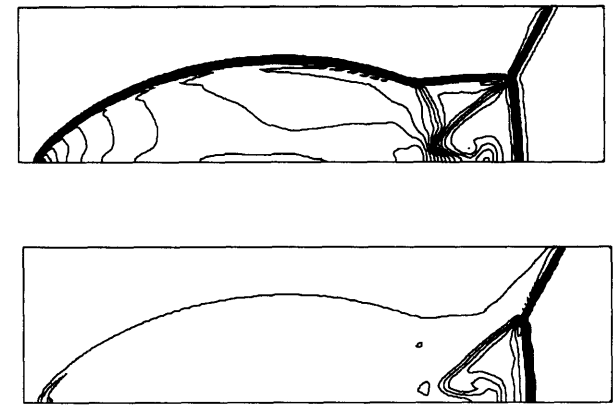

Figure 16: Double Mach Reflection (CUSP-ELED, Density and Entropy)

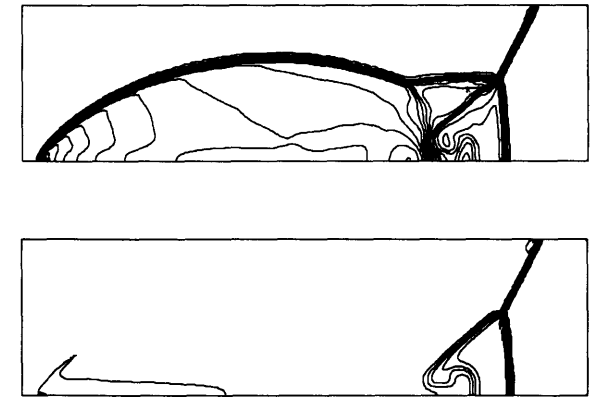

Figure 17: Double Mach Reflection (HLL-LED, Density and Entropy)

Figure 18: Double Mach Reflection (HLL-ELED, Density and Entropy)

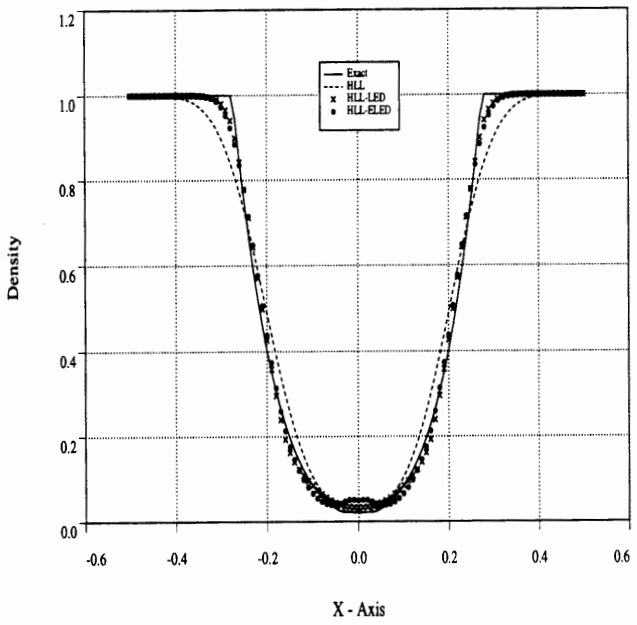

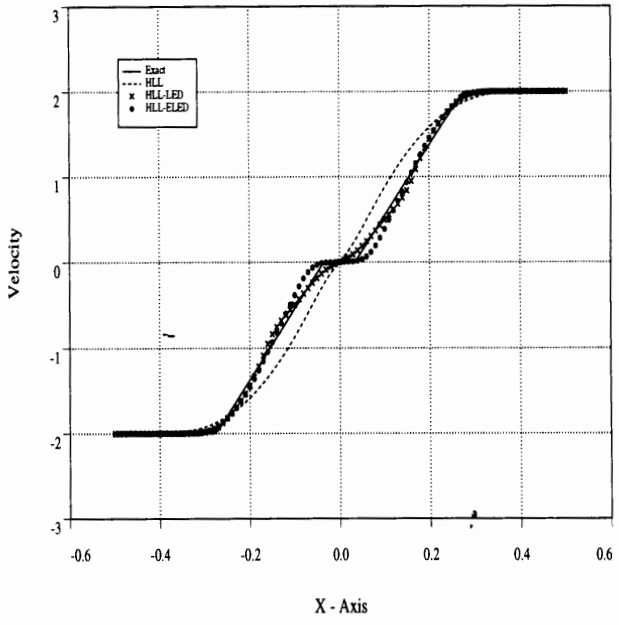

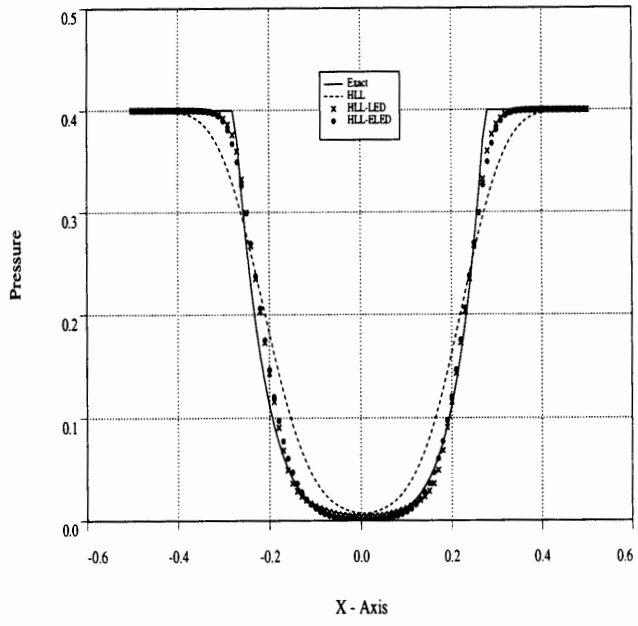

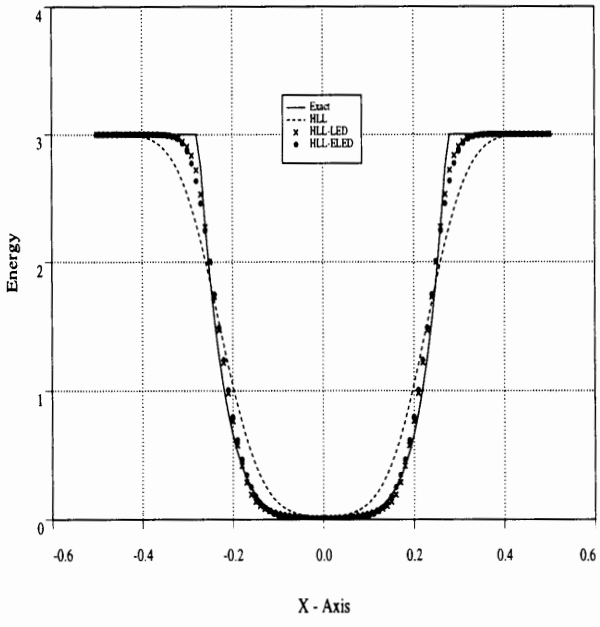

Figure 19: Supersonic Expansion (Density and Pressure)

Figure 20: Supersonic Expansion (Velocity and Energy)